Copper–cobalt alloy electrodeposition from thiocyanate solutions
1. Copper electrodeposition onto gold and copper electrodes

Antanas Steponavičius, Dijana Šimkūnaitė, Gitana Macytė and Ignas Valsiūnas

Institute of Chemistry, A. Goštauto 9, LT-2600 Vilnius, Lithuania

The voltammetric characteristics of Cu electrodeposition onto polycrystalline Au and Cu-covered Au electrodes and the initial stages of Cu electrocrystallization from nearly neutral 0.05 M Cu(I) + 3 M KSCN solution at 20 °C were investigated using linear sweep voltammetry and a potential step technique. The composition of Cu thiocyanate solution was also determined.

$Cu(SCN)^-_2$ was shown to be the predominant Cu(I) complex species. It was obtained that the discharge of the electroactive Cu(I) thiocyanate species at the Au and at Cu-covered Au electrodes was similarly irreversible. At the same time, it was suggested that a certain adsorption and/or catalytic contribution into the overall cathodic process could be also highly possible. The initial stages of electrocrystallization of Cu onto a gold substrate were shown to be rather well described by the Scharifker and Hills model involving the progressive 3D nucleation and diffusion-controlled growth. The average value of the diffusion coefficient D for Cu(I) thiocyanate species was established using the chronoamperometric results and was obtained to be equal to $1.3 \cdot 10^{-6}$ cm^2 s^{-1}. The experimental value of the stationary nucleation rate I_{st} was obtained to be equal to $6.6 \cdot 10^3$ cm^{-2} s^{-1}.

Key words: copper, thiocyanate solution, polycrystalline Au electrode, Cu-covered electrode, voltammetric results, initial stages of electrocrystallization

INTRODUCTION

Both the electrochemical behaviour of the thiocyanate anion itself and the reduction of metal thiocyanate complexes at various substrates have been studied rather intensively for a long time. As an illustration we can mention the following systems: Cu/Cu(I) [1–6], Hg/Zn(II) [7], Ag/Ag(I) [8–10], In/In(III) [10], Hg/Cd(II) [11], Hg/Fe(III) [12], Hg/Hg(II) [13, 14], Hg/Co(II) [15–19], Hg/Co(III) [17], Hg/Cr(III) [20], etc.

It seems that such a wide application of SCN^--containing systems may be associated with some interesting properties of this ligand. In particular, for investigation of the dynamics of the interfacial region, it is advantageous to use pseudohalide ion species (*e.g.,* cyanide or thiocyanate) as specific adsorbates on the electrode surface. The reason for this is that the available double-layer region is much wider in pseudohalide systems than in other cases (*e.g.,* CO). It has been established that SCN^- bonds strongly to Au [21–23] and to other metal surfaces, *e.g.,* Pt [21, 24–26], Ag [21], Hg [27, 28], Cu [22, 29]. A potential-dependent reorientation of the SCN^- ion has been shown to be possible on the Au electrode [21–23]. It has been found by *in situ* IR and SERS techniques that in almost neutral unbuffered solutions the adsorption of thiocyanate on Au occurs mainly via the sulphur atom, whereas at more negative potentials the N-bound thiocyanate could be observed to some extent [21, 22]. In an alkaline solution, mainly the S-bound thiocyanate has been observed with SERS even at negative Au electrode potentials [23]. A higher hydroxide ion concentration results in a lower bond strength between the Au surface and the adsorbed thiocyanate ion. There is a difference in the calculated binding energies for the adsorbed SCN^- at Au: 1.42 and 1.51 eV for the S-down SCN^-_{ads} and the N-down SCN^-_{ads} species, respectively [21]. It has also been proposed that thiocyanate appears to bind ionically on Au [21].

Secondly, thiocyanate has been found to exhibit a catalytic effect on the reduction of some metal ions at Hg electrode, *e.g.,* Ni(II) [30], Co(II) [15–19], Fe(II) [19, 31], Cr(III) [20], etc. and on the reduction of some non-metallic substances, *e.g.,* Cu_2Se and Cu_2S immobilized on a GC electrode [32]. The mechanism of the catalytic action of SCN^- ions, which involves the cyclic regeneration of Ni(II) or Co(II) ions by the oxidation of electrodeposited metallic Ni or Co with thiocyanate has been proposed in [17, 30]. Hydrogen ions act as a neutralizing agent of the reduction products of thiocyanate ions, cyanide and sulphide ions [17, 30]. Later, it has been found that the reduction and reoxidation of Co(II) in thiocyanate solution can be accelerated by trace amounts of cyanide and sulphide ions [18, 33] which are produced during electroreduction of Co(II). The mechanisms of the decrease in the overpotential of reducing metal thiocyanate complexes have briefly been overviewed in [19] where the formation of a solid phase of sulphides of Fe, Ni and Co on the Hg surface as the depolarizing factor has been strongly underlined.

The catalytic action of adsorbed SCN^- on the reduction of Cr(III) [20] and on the electron transfer from GC electrode to solid Cu_2Se or Cu_2S particles [32] is supposed to arise from a bridging effect.

Thirdly, as mentioned above, several metal electrodes, including Cu [22, 29, 34–36], have been shown to exhibit a tendency towards the binding of SCN^-. Thus, the formation of semiconductor cuprous thiocyanate films on Cu in KSCN solutions at open circuit or at controlled potentials (mainly in anodic region) is of interest, especially when cyclic voltammetry is used. It has been reported that during the potential sweep the initial reaction is the formation of a CuSCN monolayer [34]:

$$Cu + SCN^- \rightarrow CuSCN + e. \quad (1)$$

As the potential is increased, the monolayer formation is followed by the growth of a porous 3D CuSCN film [34]:

$$n\text{CuSCN} \rightarrow (\text{CuSCN})_n. \quad (2)$$

At positive and negative scans, the corresponding current peaks have been observed [36].

The Raman data have indicated the dominant component to be photoactive α-CuSCN in the potentiostatically formed film (nα-CuSCN is a white solid consisting of a 3D skeletal framework of mutually interlinked CuSCN molecules) and the $(CuSCN)_n$ aggregates to be preponderant in the films generated at open circuit [36]. At potentials negative of –0.65 V (*vs*. Ag/AgCl/3M KCl), both films have been found to be stripped off (0.7 M acetic acid + 0.3 M KSCN solution, pH ~3.5, 2 mV s^{-1}). The $(CuSCN)_n$ signal decays at a more negative E than the one corresponding to the α-CuSCN [36].

Fourthly, the electrochemical behaviour and voltammetric characteristics of the system Cu/Cu(I) in thiocyanate solutions are not yet clearly understood. Accumulation of thiocyanate on Cu and its incorporation into the Cu deposit have been established in alkaline 5 M KSCN + 1 M Cu(I) solution at 20 °C using a radiotracer technique [37]. The potentiodynamic behaviour of the Cu electrode under conditions of a linear potential scan in the range of $5 \cdot 10^{-3}$ to 100 V s^{-1} has been shown to differ from that for the uncomplicated reversible or irreversible discharge of thiocyanate Cu(I) complexes [5]. The peculiarities of the potentiodynamic voltammograms and the X-ray photoelectron spectroscopical data have been analyzed with respect to adsorption phenomena involved in the overall cathodic process [6]. Among the non-metallic substances, Cu_2O and Cu_2S have been shown to be present in the surface layer of the Cu deposit [6].

Finally, it seems reasonable to refine our understanding of the mechanism of electrode reactions in the metal complex systems in the general sense.

The purpose of this work was to investigate the voltammetric and chronoamperometric characteristics of Au and Cu-covered Au electrodes in an almost neutral Cu(I) thiocyanate solution. The electrolysis was carried out at a controlled potential.

EXPERIMENTAL

The working solution was 0.05 M Cu(I) + 3 M KSCN, which was prepared from doubly distilled water, CuSCN (analytical grade) and KSCN (chemically pure) in the following way. CuSCN salt was dissolved in the KSCN solution while boiling, until complete dissolution of CuSCN. Both thiocyanate salts were used as received. The solution pH was 5.8 ± 0.1. Prior to each experiment, the working solution was deaerated with purified Ar gas for 0.5 h.

All experiments were performed at 20 ± 0.1 °C in a conventional three-electrode thermostated electrochemical cell. The working electrodes were: (i) a vertical disc made from polycrystalline Au (99.95% purity) with a Teflon sheath (an exposed area was 0.5 cm^2); (ii) the same electrode covered by an electrolytic Cu layer from acidic $CuSO_4$ solution (in the text and Figures marked as (Au)Cu). The real surface area of the Au electrode was estimated from a surface gold oxide reduction charge, which was obtained by integrating the cathodic current peak in the I *vs.* E curve recorded in 0.5 M H_2SO_4 solution

at 50 mV s^{-1} in the E interval from +1.80 to +0.20 V. The charge Q_c was calculated using the cathodic-going curve, which was recorded after 10 repetitive cycling sweeps followed by holding the Au electrode at E = +1.80 V for a time required to achieve a constant value of I (particularly, for 5 min, as proposed in [38]). The value of E = +1.80 V is known to correspond to a so-called Burshtein minimum of Au electrode [39]. The charge of surface gold oxide monolayer formation or reduction (one O atom per one Au atom) was taken as 400 μC cm^{-2}, as proposed in [39]. The corrected background value of Q_c was *ca*. 0.5 mC, which yielded the roughness factor (f) equal to 2.5 ± 0.05. The counter-electrode was a Cu sheet of *ca*. 4 cm^2 in the area. The reference electrode was a Ag/AgCl/KCl (sat.) electrode. In the text, all potentials were recalculated with respect to the standard hydrogen electrode (SHE).

Prior to the first use, the Au electrode was polished mechanically using various diamond pastes of a decreasing grade from 1 μm down to 0.1 μm. Before each electrochemical experiment, the working Au electrode was pre-treated as follows: (i) immersion into HNO_3 (1:1) for 1 min followed by rinsing in doubly distilled water; (ii) light polishing with MgO followed by rinsing; (iii) immersion into HCl (1:1) followed by rinsing. Between the measurements, the working Au electrode was kept in doubly distilled water.

The electrochemical experiments were carried out using a model PI 50–1 potentiostat interfaced through a home-made analogue to digital converter with a PC (Siemens), and a PR-8 programmer and/or a PDA-1 XY-recorder. The I/E voltammograms recorded under conditions of linear potential scan or cyclic triangular potential scan and also the I/t chronoamperograms were either plotted on the XY-recorder or imported into the PC. The experimental data acquisition was in a numerical form with time resolution 50 ms per point.

In the potentiodynamic experiments, the potential was swept singly or repetitively, starting with E_{start} to the negative direction. The potential scan rates were from 0.5 to 100 mV s^{-1}.

In the chronoamperometric measurements, the I/t traces were recorded starting with E_{start} to various deposition potential E_{dep} situated in the Cu overpotential deposition (OPD) region. In all cases, before electrolysis the working electrode was potentiostatically allowed to stand at E_{start} for 1 min.

The Nernstian potential (E_{eq}) for a couple $Cu/Cu^+,SCN^-$ was evaluated: (i) by measuring an open-circuit potential ($E_{i=0}$) of Cu in the working solution, $E_{i=0}$ was found to be equal to *ca*. –0.36 V, and (ii) by equating E_{eq} to the value of the crossover potential (E_c) recorded at the lowest scan rate, the value of E_c was found to be about –0.38 V.

RESULTS AND DISCUSSION

CV characterization of the Au electrode. The working Au electrode was characterized by cyclic voltammetry in 0.5 M H_2SO_4 and in 3 M KSCN solutions.

Repetitive cyclic voltammograms of the Au electrode in 0.5 M H_2SO_4 solution showed that actually no faradaic processes occurred in the potential region +0.20 to +1.34 V during the positive-going scans – the current was due to the double-layer charging (Fig. 1). Rather unusually large background currents in this E region, *i.e*. at E positive of *ca*. +0.80 V here, have already been observed in some media, including the acidic one [40]. Such a phenomenon has been explained by the formation of a sub-monolayer (10–20% coverage) of specifically adsorbed water as a discharged species when the acidic solution has been applied for the experiments.

It can be seen from Fig. 1 that the oxidation of the Au surface occurs during the positive-going potential scan more positive than +1.34 V up to the potential of the current minimum just before the oxygen evolution and the formation of other Au oxygenated compounds, *i.e*. up to the so-called Burshtein minimum. This resulted in the formation of a surface gold oxide monolayer [39, 41, 42]. The corresponding reduction of this monolayer of the surface gold oxide occurs in the subsequent negative-going potential scan. The integration of the charge for oxide reduction was used here to estimate the roughness factor of the Au electrode surface, as noted above.

Repetitive cyclic voltammetry applied to Au in the blank solution of 3 M KSCN showed that the currents observed in the almost stabilized CV, *e.g*.

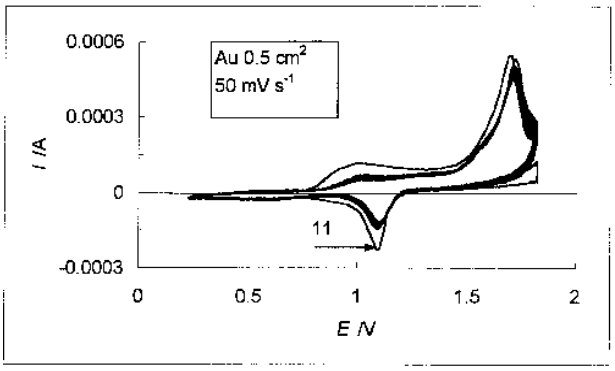

Fig. 1. Repetitive cyclic voltammograms for polycrystalline Au electrode in 0.5 M H_2SO_4 solution in the potential range +0.20 to 1.80 V (10 cycles). The real surface area of the Au electrode was evaluated from CV recorded by the 11th sweep as noted in the text

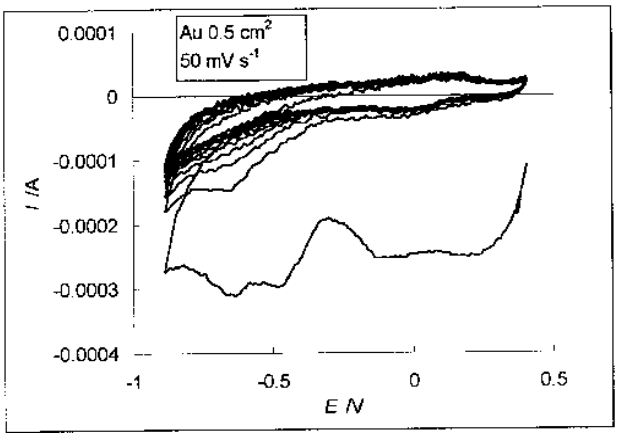

Fig. 2. Repetitive cyclic voltammograms for polycrystalline Au electrode in 3 M KSCN solution (10 cycles)

at the 10th sweep (Fig. 2), did not exceed *ca*. $1 \cdot 10^{-4}$ A in the cathodic half-cycle and $5 \cdot 10^{-5}$ A in the anodic one.

Composition of near-neutral Cu(I) thiocyanate solution. It has been known that Cu^+ ions, like other metal ions of the d^{10}-system, form complexes with SCN^- through a metal-S bond (see, *e.g.*, [43, 44]). As mentioned above, the complex system Cu^+–SCN^- has already been studied in several works [1–5]. The complex species have been shown to be $Cu(SCN)_4^{3-}$ [1] or $Cu(SCN)_n^{1-n}$, where n = 3, 4, 5 or 6 [3]. Taking into consideration not only the data reported in [3], but also the data summarized in [45, 46], the parameter n was taken here to be equal to 2, 3, 4, 5, 6. In view of a near-neutral medium, the protonation of thiocyanate can be not accounted for. Then, following a procedure presented in [4, 47], the distribution of the species in the solution was calculated using the values of cumulative stability constants as follows: log β_2 = 12.11, log β_3 = 9.9, log β_4 = 10.09, log β_5 = 9.59 and log β_6 = 9.27 [45, 46]. The results of the calculation of the distribution of various species in 0.05 M Cu(I) solution depending on the concentration of KSCN are presented in Fig. 3. One can see that under conditions of our experiment, the particle $Cu(SCN)^-_2$ is the predominant complex species.

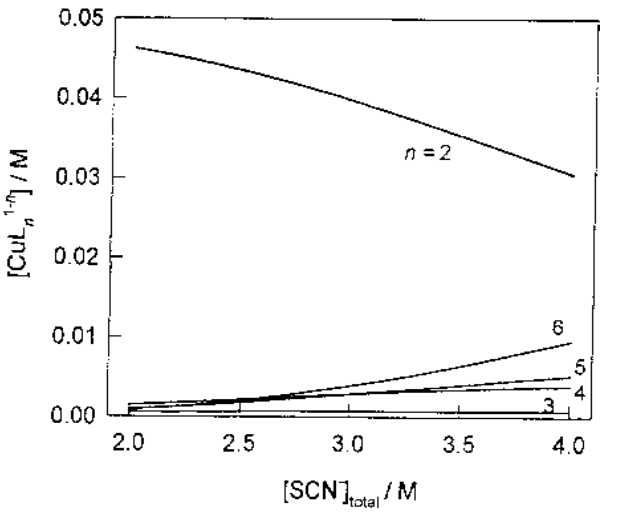

Fig. 3. Distribution of the equilibrium concentrations of Cu(I) thiocyanate complexes calculated for 0.05 M Cu(I) + + x M KSCN solution at pH 5.8 and a temperature of 20 °C

As regards the possibility of the formation of Cu_2O, the calculation of the maximum value of the equilibrium concentration of Cu^+ when the formation of Cu_2O does not yet occur ($[Cu^+]_{max}$) showed that this quantity estimated according to the equation [48]

$$\log [Cu^+]_{max} = -0.84 - pH \qquad (3)$$

is equal to *ca*. $2.3 \cdot 10^{-7}$ mol l^{-1}. On the other hand, the calculated concentration of Cu^+ as one of the particles existing in the thiocyanate solution was obtained to be equal to $3.31 \cdot 10^{-15}$ mol l^{-1}, *i.e.* it was far below the value of $[Cu^+]_{max}$. So, the formation of low-soluble Cu_2O is not expected to form as a bulk phase.

Voltammetry of Au electrode in Cu(I) thiocyanate solution. The voltammetric responses (the 1st scan) recorded on the Au surface from 3 M KSCN + + 0.05 M Cu(I) solution at various scan rates (v) are presented in Fig. 4. This figure shows that each of the cyclic voltammograms (CVs) exhibits a single cathodic current peak and a single anodic one. The cathodic current peaks at the peak potentials (E_{pc}) in the range –0.45 to –0.49 V can be assigned to the Cu overpotential deposition. The onset of this process occurs at about –0.40 V. Then, the anodic current peaks should correspond to the Cu stripping process. As mentioned above, the open-circuit potential ($E_{i=0}$) can be taken in this work as a reversible potential for the couple Cu/Cu(I) (E_{eq}), thus allowing evaluation of the Cu deposition overpotential (η_c).

The run of the cathodic branches of the CVs lying between E_{start} and the onset of the bulk Cu deposition was not considered here because of a rather rough current scale used for the experiments.

It should be pointed out that no "nucleation loops" in the CVs were observed after scan reversal (Fig. 4). As is known [49, 50], such current excursions are usually associated with the nucleation/growth rate controlled electrodeposition processes, when the scans have been reversed prior to intercrystal collisions. Most likely the absence of the "nucleation loops" in the experimental CVs (Fig. 4) can be explained by the scan reversal not satisfying this requirement.

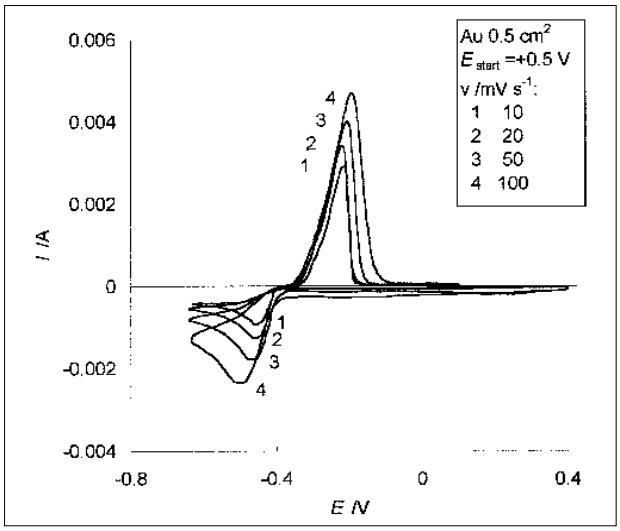

Fig. 4. Typical cyclic voltammograms for copper deposition on the polycrystalline Au electrode from 0.05 M Cu(I) + + 3 M KSCN solution at various potential scan rates v. The 1st scan to negative direction

The cathodic current peak (I_{pc}) was found to increase with v. The dependence of I_{pc} against v was plotted here in double logarithmic coordinates, *i.e.* log I_{pc} *vs.* log v (Fig. 5*a*). As can be seen, the slope of this linear dependence is about 0.43. Although the experimental value of the parameter dlog I_{pc}/dlog v is slightly less than the quantity 0.5 expected for a diffusion-controlled electrochemical reaction [51], it can be formally concluded that the cathodic current peak height is determined predominantly by diffusion.

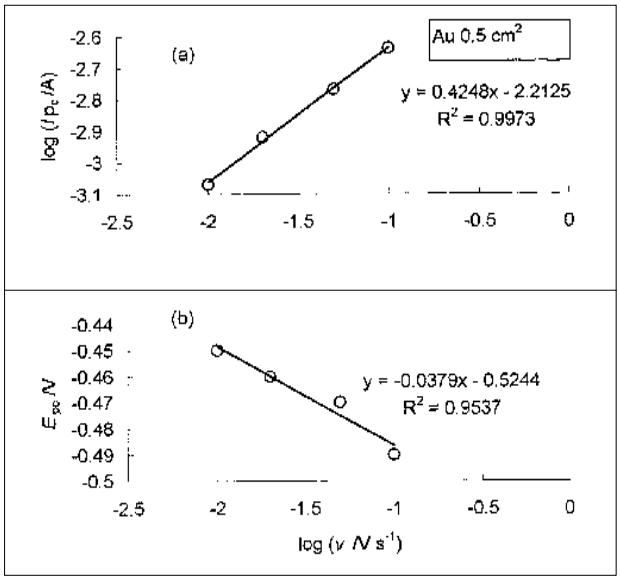

Fig. 5. Variation of current peak I_{pc} (*a*) and peak potential E_{pc} (*b*) with potential scan rate v (from the results in Fig. 4)

To distinguish the cases of reversible and totally irreversible charge transfer taking place during reduction at a planar electrode under the potentiodynamic conditions, along with the dependence I_{pc} against v, other parameters of CVs can also be used [51, 52]. Among them, the peak potentials (E_{pc}) and the shape of the experimental CVs provide the most important information [51, 52].

The peak potential E_{pc} was shifted negatively when v was increased, as shown in Figs. 4 and 5*b*. This feature of the CVs excluded the case of the reversible charge transfer. The slope of E_{pc} *vs.* log v plot was found to be close to –0.038 V dec^{-1}. According to [51, 52], for a totally irreversible potentiodynamic wave a shift in E_{pc} at 20 °C is about $30/\alpha_c n_\alpha$ millivolts for each ten-fold increase in v. Then, taking the electron-transfer number for the reduction of the Cu(I) thiocyanate complexes $n_\alpha = 1$ and a transfer coefficient $\alpha_c = 0.5$, the shift in E_{pc} of about 60 mV dec^{-1} is to be expected. As is obvious, there is a significant difference between the experimental and the expected values of the parameter dE_{pc}/dlog$v$ (the latter quantity for the case of totally irreversible charge transfer). The lesser value of the experimental value of the slope E_{pc} *vs.* log v plot (Fig. 5*b*) than the theoretical one, *i.e.* a significantly higher value of α_c obtained as compared with 0.5, is as yet difficult to explain. It should be added that the case of a coupled chemical reaction preceding a charge transfer is perhaps unreasonable, as followed from the calculation of the distribution of the species in the working Cu(I) thiocyanate solution (see above).

To check whether adsorption of reagents has an effect upon the overall electrode process under examination, according to [53–55] we further considered the scan rate-dependences of some current functions, *viz.* $I_{pc}/v^{0.5}$ and I_{pc}/v. It is known (see, *e.g.*, [54]) that the scan rate is probably the most important experimental parameter for differentiating between the effects caused by adsorbed reactants and those evoked by material arriving at the electrode by diffusion. As can be seen from the diagram presented in Fig. 6*a*, dependence of the current function $I_{pc}/v^{0.5}$ on log v can be reasonably well approximated by a straight line with a rather insignificant negative slope indicating only a weak adsorption of the reagent to be expected, in line with the criterion in [53–55]. Relating the dependence of another current function on v, *i.e.* I_{pc}/v *vs.* v, it is evident (Fig. 6*b*) that the quantity I_{pc}/v decreases with increasing v and that this dependence fits quite well the equation $I_{pc}/v = 0.0051v^{-0.62}$. In accordance with the considerations presented in [53–55], it follows that, in the range of larger values of v where I_{pc}/v is almost independent of v, a surface process can be expected (Fig. 6*b*). In the range of lower values of v, where

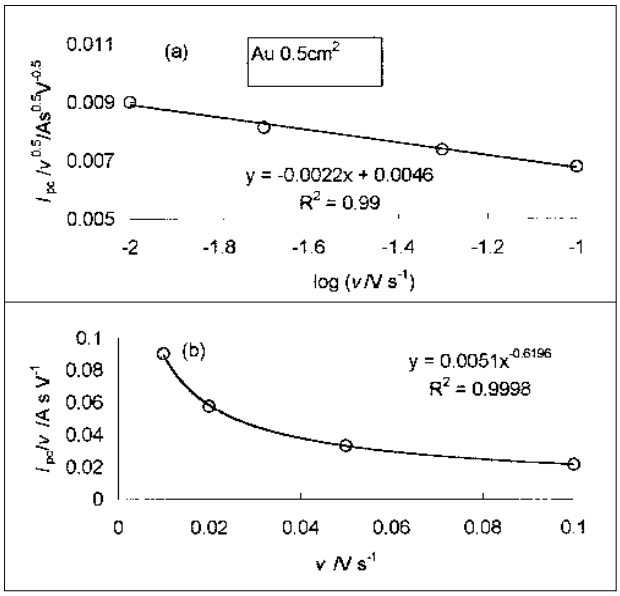

Fig. 6. Variation of current peak functions $I_{pc}/v^{0.5}$ (*a*) and I_{pc}/v (*b*) with potential scan rate v (from the results in Fig. 4)

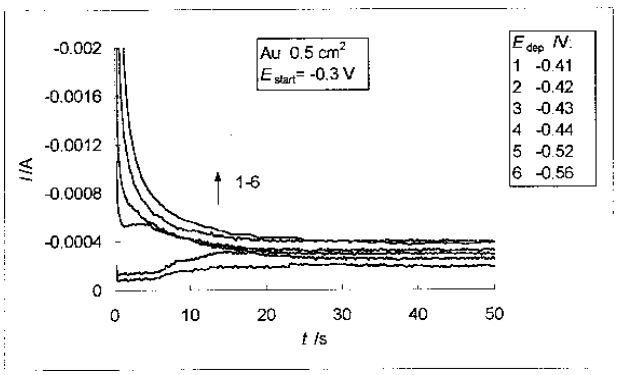

Fig. 7. Potentiostatic I *vs.* t transients of polycrystalline Au electrode in 0.05 M Cu(I) + 3 KSCN solution, recorded after stepping the potential from the starting potential E_{start} to various Cu deposition potential E_{dep}

the amount of diffusing material is higher relative to the amount of adsorbed material reacting at the electrode surface, the effect of the adsorption phenomena is not revealed (Fig. 6*b*).

So, considering the voltammetric features discussed above, it can be concluded that the electrodeposition of Cu onto Au from a nearly neutral Cu(I) thiocyanate solution is probably an irreversible electrode reaction which under the potentiodynamic conditions becomes diffusion-controlled. Besides, the overall process includes contributions of other phenomena. Although our results give no sufficient evidence for selecting one of them, it is suggested that a weak adsorption of reagents can be expected. The increase in the value of v seems to be favourable for revealing the adsorption phenomena.

Chronoamperometric results. The nucleation and growth of Cu during electrodeposition on the polycrystalline Au electrode from a nearly neutral Cu(I) thiocyanate solution were studied by the potential step technique. Figure 7 shows a set of cathodic current transients recorded starting from E_{start} = = –0.30 V to various deposition potentials E_{dep}. Most of these transients are typical of a diffusion-controlled process of 3D nucleation and growth of a metal deposit on a foreign substrate [56–58]. First, they have a sharp current spike due to charging the double layer [56]. This capacitive part of the transient is followed by a rise in the current due to an increase in the effective electrode area as the nuclei form and grow in size [56–58]. The current reaches the maximum (I_{max}) as the hemispherical diffusion zones radiating from each growing nucleus begin to overlap and the hemispherical mass transfer becomes a semi-infinite linear diffusion to a planar surface of the electrode. Finally, at $t > t_{max}$, a rather slow decrease in the current should be typical of an electrode reaction limited by a semi-infinite linear diffusion of the discharging ions, and the current–time relation should follow the Cottrell relationship [56–58].

Several models have been developed for the 3D nucleation and growth phenomena taking place during bulk metal deposition on a foreign substrate [56–58]. The models involving two limiting cases of the 3D nucleation processes, instantaneous and progressive, in conjunction with the hemispherical diffusion-controlled growth of nuclei formed have been found to be most appropriate for analyzing the initial stages of electrocrystallization.

The best known method for differentiating the two nucleation models is to compare the experimental dimensionless current–time transients to the theoretical dimensionless transients for each nucleation mechanism [56–58]. The following theoretical equations have been proposed [56] for instantaneous (4) and for progressive (5) nucleation:

$$(I/I_{max})^2 = 1.9542(t/t_{max})^{-1}\{1-\exp[-1.2564(t/t_{max})]\}^2 \quad (4)$$

$$(I/I_{max})^2 = 1.2254(t/t_{max})^{-1}\{1-\exp[-2.3367\,(t/t_{max})^2]\}^2. \quad (5)$$

These equations correlate the dimensionless current I/I_{max} to the dimensionless time $t/t_{max.}$

The experimental plots, $(I/I_{max})^2$ *vs.* (t/t_{max}), obtained for some values of E_{dep}, along with the theoretical plots resulting from Eqs. (4) and (5), are shown in Fig. 8. These plots suggest that Cu deposition onto a polycrystalline Au electrode from a nearly neutral Cu(I) thiocyanate solution agrees rather well

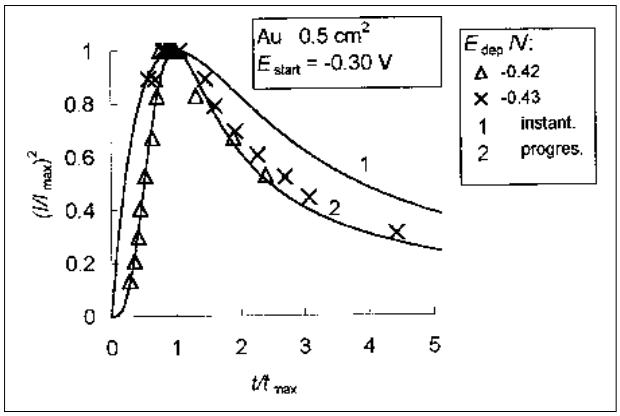

Fig. 8. Comparison of the experimental Cu nucleation onto the polycrystalline Au electrode from 0.05 M Cu(I) + 3 M KSCN solution to the corresponding theoretical nucleation processes [54]

with the limiting model of progressive 3D nucleation. However, under these conditions the region of E_{dep} applied for obtaining the transients suitable for further analysis is narrow.

Once it is established that the nucleation is progressive, it is possible to get information about the diffusion coefficient (D) of the electroactive species from the maximum of the I/t transients in the case of progressive nucleation via the equation [56]:

$$I^2_{max} \cdot t_{max} = 0.2598(zFc)^2D. \quad (6)$$

Taking here the valence $z = 1$ and the concentration of Cu(I) $c = 5 \cdot 10^{-5}$ mol cm^{-3} and also using the current density maximum to the whole Au electrode surface instead of the current maximum, from a single experimental point ($I_{max,}$ t_{max}) at the selected value of the E_{dep}, *e.g.*, at –0.41 V, it was obtained that the calculated average diffusion coefficient D was about $1.3 \cdot 10^{-6}$ cm^2 s^{-1}.

Using a single experimental point (I_{max}, t_{max}), it is also possible to evaluate the stationary nucleation rate (I_{st}), as is shown in Ref. [59]. The method to obtain this parameter has been proposed to be as follows. According to [57], the progressive cathodic $I(t)$ relationship and the coordinates (I_{max}, t_{max}) of the maximum of the progressive current transient are given, respectively, by:

$$-I(t) = (zFcD^{1/2}/(\pi t)^{1/2}) \cdot [1-\exp(-0.5I_{st}\pi k'Dt^2)], \quad (7)$$

$$-I_{max} = 0.46\ zFSc(D^3k')^{1/4}I^{-1/2}_{st}, \quad (8)$$

$$t_{max} = 2.16(\pi k'D)^{-1/2}\ I^{-1/2}_{st}, \quad (9)$$

where z is the valence, $k' = (4/3)(8\pi c v_m)^{1/2}$, v_m is the molar volume of the deposit. Then, the product $I_{max} \cdot t^{1/2}_{max}$ can be given by [59]:

$$-I_{max} \cdot t^{1/2}_{max} = 0.9032S\pi^{-1/2}zFcD^{1/2}. \quad (10)$$

From Eqs. (7) and (10) one can obtain:

$$-\ln M = Qt^2, \quad (11)$$

where

$$M = 1 - 0.9032It^{1/2}/I_{max} \cdot t^{1/2}_{max}, \quad (12)$$

and

$$Q = 0.613\pi^2k't_{max}I^2_{max}I_{st}/(zFSc)^2. \quad (13)$$

So, from Eq. (11) it follows that the I/t transient should be transformed into a straight line passing through the origin. The nucleation rate I_{st} could be determined from the slope Q of the straight line.

Figure 9 shows a $-\ln M$ *vs.* t^2 plot obtained from the I/t transient at $E_{dep} = -0.41$ V (Fig. 7) taking $z = 1$, $c = 5 \cdot 10^{-5}$ mol cm^{-3}, $S = 0.5$ cm^2 and $v_m = 7.1$ cm^3 mol^{-1}. Since in our case the slope Q of the $-\ln M$ *vs.* t^2 plot is equal to 0.0017, the value of the stationary nucleation rate I_{st} at $E_{dep} = -0.41$ V calculated from this slope by Eq. (13) was found to be $6.6 \cdot 10^3$ cm^{-2} s^{-1}.

Finally, we have to point out that a more precise analysis of the experimental data obtained should take into account the η_c-dependence of I_{st} which was not yet considered here, and also the distribution of the surface concentrations of the Cu(I) species rather than the bulk c. In addition, it should be stressed that, to our knowledge, such an investigation of the initial stages of electrocrystallization of Cu onto a foreign substrate from a Cu(I) thiocyanate solution was made for the first time.

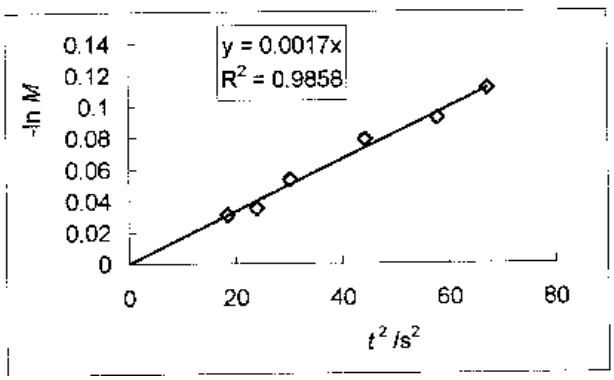

Fig. 9. $-\ln M$ *vs.* t^2 plot of the data from Fig. 7

Electrodeposition of Cu onto a Cu-covered Au electrode. Analysis of the potentiodynamic *I vs. E* curves registered with the (Au)Cu working electrode (not presented here) showed that the general shape of the curves was quite similar to that obtained with the working Au electrode (Fig. 4). Particularly, it was established that the parameter dlog I_{pc}/dlog *v* was equal to 0.48. This value is close to the value 0.5 expected for a diffusion-controlled electrochemical process [51] and also to the experimental value 0.51 obtained earlier [5]. The E_{pc} and $E_{pc/2}$ dependences on log *v* were found to be linear, as in the case of the Au working electrode. The experimental slopes of the E_{pc} *vs.* log *v* and $E_{pc/2}$ *vs.* log *v* plots (not presented here) were found to be about –0.02 V dec^{-1}, yielding formally the cathodic Tafel coefficient b_c equal to –0.04 V. It is evident that, as in the case of the Au electrode, such a value of b_c is significantly less and, correspondingly, the transfer coefficient α_c is markedly higher than the parameters expected for a pure irreversible one-electron transfer process.

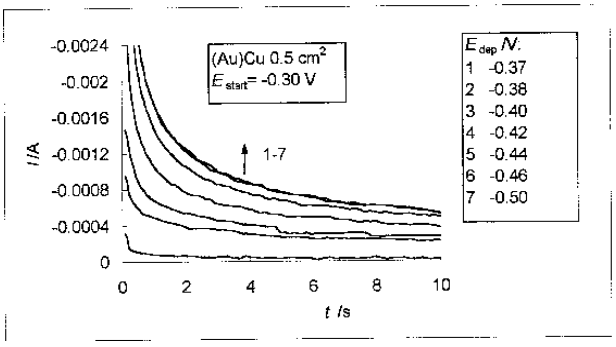

Fig. 10. Potentiostatic *I vs. t* transients of (Au)Cu electrode in 0.05 M Cu(I) + 3 M KSCN solution recorded after stepping the potential from the starting potential E_{start} to various Cu deposition potentials E_{dep}

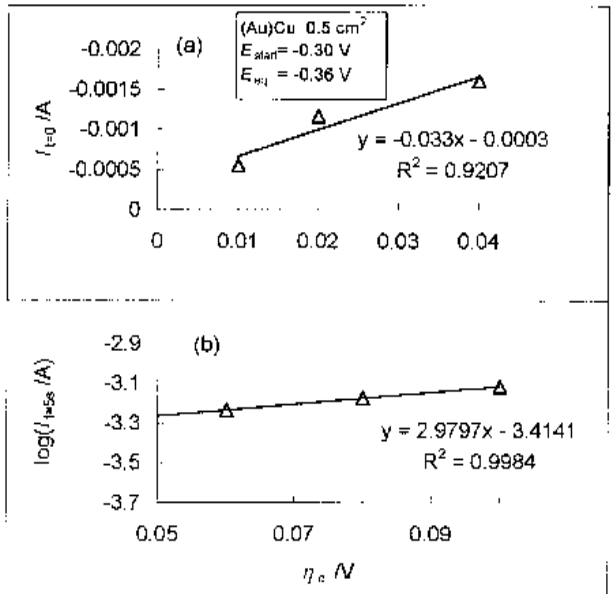

Fig. 11. $I_{t=0}$ *vs.* η_c (*a*) and log *I vs.* η_c (*b*) plots for the (Au)Cu electrode in 0.05 M Cu(I) + 3M KSCN solution (from results in Fig. 10)

To obtain a Tafel relationship log*I vs.* η_c from which b_c could be established as well, the conventional potential step technique was applied. The potentiostatic *I*/*t* transients at various E_{dep} are presented in Fig. 10. The values of *I* obtained by extrapolation of the *I vs.* $t^{0.5}$ dependences to $t = 0$ were used for preparing the $I_{t=0}$ *vs.* η_c plot in the region of small overpotentials (Fig. 11*a*), while the values of *I* fixed at $t = 5$ s were used for preparing the log *I vs.* η_c plot at higher η_c (Fig. 11*b*). In the latter case, it was assumed that the contribution of the diffusion process into the overall run of *I*(*t*) dependences at different η_c may not be significant. It can be seen from the Tafel-like plot log $I_{t=5s}$ *vs.* η_c (Fig. 11*b*) that, surprisingly, the experimental value of b_c obtained is equal to –0.336 V, *i.e.* it is quite different from that calculated from the potentiodynamic results. Such a curious difference is as yet difficult to be explained on the basis of the experimental results obtained in our study. Further, using the known equation [60]

$$I_{t=0} = I_0 nF\eta_c/RT, \qquad (14)$$

the data presented in Fig. 11*a* formally yield the value of the exchange current I_0 to be about $1.3 \cdot 10^{-3}$ A.

So, it should be concluded that the parameters of the cathodic process occurring at both the Au and (Au)Cu electrodes in Cu(I) thiocyanate solution are only apparent and do not allow an elucidation of the reaction mechanism. In our opinion, the deviation from a pure irreversible one-electron transfer reaction observed here may be caused by a contribution of a certain catalytic component, as it has been shown earlier for the case of electrodeposition of Ni, Co and Fe [19].

CONCLUSIONS

$Cu(SCN)^-_2$ has been shown to be the predominant Cu(I) complex species in the nearly neutral 0.05 M Cu(I) + 3 M KSCN solution. It has been obtained that the discharge of the electroactive Cu(I) thiocyanate species at the Au and at Cu-covered Au electrodes is perhaps irreversible. At the same time, it can be suggested that the adsorption and/or catalytic contribution into the overall cathodic process is also highly possible. The initial stages of electrocrystallization of Cu onto a gold substrate were shown

to be rather well described by the Scharifker and Hills model involving the progressive 3D nucleation and the diffusion-controlled growth. The average value of the diffusion coefficient D for Cu(I) thiocyanate species was established, using the chronoamperometric results. The experimental value of the stationary nucleation rate was obtained to be equal to $6.6 \cdot 10^3$ cm^{-2} s^{-1}, and the experimental value of exchange current was found to be about $1.3 \cdot 10^{-3}$ A.

ACKNOWLEDGEMENTS

The authors thank Prof. A. Survila for the calculation of the distribution of the equilibrium concentrations of Cu(I) complex species.

Received 15 October 2001
Accepted 17 January 2002

References

1. I. A. Korshunov and N. I. Maliugina, *Zh. obshch. khim.,* **20**, 1399 (1950).
2. A. V. Panphilov, O. E. Panchuk, and I. E. Panchuk, *Ukr. khim. zh.,* **21**, 400 (1955).
3. A. M. Golub, *Zh. neorg. khim.,* **1**, 2517 (1956).
4. A. Žukauskaitė and A. Survila, *Chemija,* Nr. **2(181)**, 31 (1991).
5. O. Girčienė, B. Šebeka, V. Kapočius, and A. Steponavičius, *Chemija,* Nr. 3, 41 (1997).
6. O. Girčienė, B. Šebeka, V. Jasulaitienė, and A. Steponavičius, *Chemija*, Nr. 3, 73 (1997).
7. R. A. Osteryoung and J. H. Christie, *J. Phys. Chem.,* **71**, 1348 (1967).
8. J. N. Pearce and L. Smith, *J. Amer. Chem. Soc.,* **59**, 2063 (1937).
9. A. Survila, G. Cesiulis, and T. Jankauskas, *Tr. AN Lit. SSR, Ser. B,* **4(149),** 11 (1985).
10. I. Krastev, M. E. Baumgärtner, and Ch. J. Raub, *Galvanotechnik*, **88**, 1882 (1997).
11. D. N. Hume, D. D. DeFord, and G. C. B. Cave, *J. Amer. Chem. Soc.*, **73**, 5323 (1951).
12. K. Ogura, T Ooeda, and T. Yoshino, *Electrochim. Acta,* **21**, 1041 (1976).
13. N. A. Kolpakova and A. I. Kartushinskaya, *Izv. Tomsk. Polytekh. Inst.,* **185,** 80 (1970).
14. A. I. Kartushinskaya, A. G. Stromberg, and N. A. Kolpakova, *Elektrokhimiya,* **7**, 1243 (1971).
15. D. J. Astley and J. A. Harrison, *Electrochim. Acta,* **15**, 2007 (1970).
16. E. Eriksrud, *J. Electroanal. Chem.,* **54**, 341 (1974).
17. E. Itabashi and M. Tan, *J. Electroanal. Chem.,* **60**, 299 (1975).
18. E. Itabashi, *J. Electroanal. Chem.,* **188**, 205 (1978).
19. K. Winkler and T. Krogulec, *J. Electroanal. Chem.,* **281**, 171 (1990).
20. M. J. Weaver and F. C. Anson, *J. Electroanal. Chem.,* **65**, 759 (1975).
21. K. Ashley, F. Weinert, and D. L. Feldheim, *Electrochim. Acta,* **36**, 1863 (1991).
22. M. Bron and R. Holze, *J. Electroanal. Chem.,* **385**, 105 (1995).
23. M. Bron and R. Holze, *Electrochim. Acta,* **45**, 1121 (1999).
24. A. Tadjeddine and P. Guyot-Sionest, *Elektrokhimiya*, **29**, 73 (1993).
25. Z. Q. Tian, B. Ren, and B. W. Mao, *J. Phys. Chem. B.*, **101**, 1338 (1997).
26. Q. Peng and J. J. Breen, *Electrochim. Acta,* **43**, 2619 (1998).
27. H. Wroblowa, Z. Kovac, and J. O'M. Bockris, *Trans. Faraday Soc.,* **61**, No. 511, Part 7, 1523 (1965).
28. R. Parsons and P. C. Symons, *Trans. Faraday Soc.,* **64**, No. 544, Part 4, 1077 (1968).
29. G. V. Korshin and M. S. Shapnik, *Elektrokhimiya,* **21**, 1203 (1985).
30. E. Itabashi, *J. Electroanal. Chem.,* **60**, 285 (1975).
31. K. Winkler, T. Krogulec, and Z. Galus, *Electrochim. Acta,* **30**, 1055 (1985).
32. B. Lange, M. Lovrić, and F. Scholz, *J. Electroanal. Chem.,* **418**, 21 (1996).
33. T. Krogulec, A. Barański, and Z. Galus, *J. Electroanal. Chem.,* **144**, 303 (1983).
34. M. G. Figueroa, R. C. Salvarezza, and A. J. Arvia, *Electrochim. Acta,* **31**, 671 (1986).
35. F. Guillaume and G. L. Griffin, *Langmuir,* **5**, 783 (1989).
36. Y. Son, N. R. de Tacconi, and K. Rajeshwar, *J. Electroanal. Chem.,* **345**, 135 (1993).
37. B. Radžiūnienė, J. Butkevičius, A. Steponavičius, and R. Višomirskis, in *Issledovaniya v oblasti osazhdeniya metallov*, Vilnius, 101 (1971).
38. K. Juodkazis, J. Juodkazytė, B. Šebeka, and A. Lukinskas, *Electrochem. Commun.*, **1**, 315 (1999).
39. A. M. Michri, A. G. Pshenichnikov, and R. Kh. Burshtein, *Elektrokhimiya,* **8**, 364 (1972).
40. G. Nguyen van Huong, C. Hinnen, and J. Lecoeur, *J. Electroanal. Chem.,* **106**, 185 (1980).
41. H. Angerstein-Kozlowska, B. E. Conway, A. Hamelin, and L. Stoicoviciu, *Electrochim. Acta*, **31**, 1051 (1986).
42. H. Angerstein-Kozlowska, B. E. Conway, A. Hamelin, and L. Stoicoviciu, *J. Electroanal. Chem*, **228**, 429 (1987).
43. Chr. K. Jørgensen, *Inorganic Complexes*, Academic Press, London-New York (1963).
44. M. C. Day and J. Selbin, *Theoretical Inorganic Chemistry* (3rd ed.), Khimiya, Moscow (1976) (in Russian).
45. L. G. Sillen (Compil.), *Stability Constants of Metal–Ion Complexes. Section I: Inorganic Ligands. (Special Publ. No. 17)*, The Chemical Society, Burlington House, London (1964).
46. Yu. Yu. Lur'e, *Reference Book on Analytical Chemistry,* Khimiya, Moscow (1989) (in Russian).
47. A. Survila, *Electrode Processes in Systems of Labile Complexes of Metals,* Mokslas, Vilnius (1989) (in Russian).
48. N. de Zoubov, C. Vanleugenhagne, and M. Pourbaix, in *Atlas of Electrochemical Equilibria in Aqueous Solu-*

tions (Ed. M. Pourbaix), Pergamon Press, Oxford–London–Edinburgh–New York–Toronto–Paris–Frankfurt, and Cebelcor, Brussels, Sect. 14.1 (1966).
49. S. Fletcher, *Electrochim. Acta*, **28**, 917 (1983).
50. S. Fletcher, C. S. Halliday, D. Gates, M. Westcott, T. Lwin, and G. Nelson, *J. Electroanal. Chem.,* **159**, 267 (1983).
51. R. S. Nicholson and I. Shain, *Analyt. Chem.,* **36**, 706 (1964).
52. H. R. Thirsk and J. A. Harrison, *A Guide to the Study of Electrode Kinetics,* Academic Press, London–New York (1972).
53. V. D. Parker, in *Comprehensive Chemical Kinetics* (Eds. C. H. Bamford and R. G. Compton). Vol. 26 – *Electrode Kinetics: Principles and Methodology,* p. 145, Elsevier, Amsterdam–Oxford–New York–Tokyo (1986).
54. R. H. Wopschall and I. Shain, *Analyt. Chem.,* **39**, 1514 (1967).
55. S. Srinivasan and E. Gileadi, *Electrochim. Acta,* **11**, 321 (1966).
56. B. Scharifker and G. Hills, *Electrochim. Acta,* **28**, 879 (1983).
57. G. Gunawardena, G. Hills, I. Montenegro, and B. Scharifker, *J. Electroanal. Chem.,* **138,** 225 (1982).
58. B. Scharifker and J. Mostany, *J. Electroanal. Chem.,* **177**, 13 (1984).
59. A. Kelaidopoulou, G. Kokkinidis, and A. Milchev, *J. Electroanal. Chem.* **444**, 195 (1998).
60. B. B. Damaskin and O. A. Petrii, *Introduction to Electrochemical Kinetics,* p. 277, Vysshaya shkola, Moscow (1975) (in Russian).

A. Steponavičius, D. Šimkūnaitė, G. Macytė, I. Valsiūnas

VARIO–KOBALTO LYDINIO ELEKTROLITINIS NUSODINIMAS IŠ TIOCIANATINIŲ TIRPALŲ
1. VARIO ELEKTROLITINIS NUSODINIMAS ANT AUKSO IR VARIO ELEKTRODŲ

S a n t r a u k a

Linijinio potencialo skleidimo ir potenciostatinio įjungimo metodais buvo tiriamos Cu elektrolitinio nusodinimo ant polikristalinio Au ir variu padengto Au elektrodų voltamperinės charakteristikos ir Cu elektrokristalizacijos pirmosios stadijos ant Au substrato beveik neutraliame 0,05 M Cu(I) + 3 M KSCN tirpale esant 20°C temperatūrai. Taip pat buvo nustatyta Cu(I) tiocianatinių tirpalų sudėtis.

Parodyta, kad kompleksas $Cu(SCN)^{-}_{2}$ yra vyraujanti Cu(I) kompleksinė dalelė. Nustatyta, kad elektrochemiškai aktyvių Cu(I) tiocianatinių dalelių išsikrovimas ant Au ir ant variu padengto Au elektrodų, matyt, yra negrįžtamas. Manoma, kad tam tikrą indėlį į bendrą katodinį procesą gali įnešti adsorbciniai ir/ar elektrokataliziniai reiškiniai.

Cu elektrokristalizacijos ant Au paviršiaus pirmosios stadijos gana gerai aprašomos Scharifker ir Hills pasiūlytu progresuojančiu 3D kristalų užuomazgų susidarymo ir difuzijos kontroliuojamo tolesnio jų augimo modeliu. Panaudojus chronoamperometrinių tyrimų rezultatus, įvertintas vidutinis Cu(I) tiocianatinių dalelių difuzijos koeficiento dydis. Jo reikšmė yra $1{,}3 \cdot 10^{-6}$ cm^2 s^{-1}. Nustatyta, kad pastovusis kristalų branduolių susidarymo greitis I_{st} yra $6{,}6 \cdot 10^{3}$ cm^{-2} s^{-1}.